

IACHEC Legacy Working Group White Paper

IACHEC-LWG-WP-0001

A synoptic view of X-ray in-flight calibration plans

Matteo Guainazzi (*Astro-H and XMM-Newton SOC, ESA-ESAC, Villafranca del Castillo, Spain*)

May 8, 2014

History

Version	Date	Editor	Note
0.1	May 8, 2014	Matteo Guainazzi	First version with complete text

List of acronyms

- CTI: Charge Transfer Inefficiency
- GBH: Galactic Black Hole
- IACHEC: International Astronomical Consortium for High-Energy Calibration
- INS: Isolated Neutron Star
- LSF: Line Spread Function
- PWN: Pulsar Wind Nebula
- PSF: Point Spread Function
- SNR: Super-Nova Remnant
- WD: White Dwarf
- WG: Working Group

1 Scope of this document

Ideally, calibration of space X-ray instruments is the result of a complete physical model supported by an adequate set of ground-based measurements under controlled conditions. Regrettably, time and budget pressure during the mission development phase, as well as the degradation of the instrument performances in space (radiation damages, contamination, electronic failures) more often than not impose a throughout re-calibration using celestial sources. “In-flight” calibration programs have been playing a crucial role in our understanding of the instrument scientific performances, as well as (and, often, more crucially) of their time evolution.

While X-ray astronomy is nowadays a fully mature and globally integrated science, calibration of X-ray space instruments was carried out for decades in isolation, and with little cross-talk among calibration teams of different instruments and know-how transfer from older to newer mission (besides the natural transfer of calibration scientists to newer projects). This has led to a wide variety of approaches in dealing with similar calibration issues over different missions, as well as to a surprisingly large variety of celestial sources being used for the same calibration purpose.

The birth of the *International Astronomical Consortium for High-Energy Calibration* (IACHEC; <http://web.mit.edu/iachec/>; Sembay et al. 2010) in 2006 tried and alleviate this original sin, by achieving a better integration among calibration activities of operational high-energy observatories. In this context “*The IACHEC aims to provide standards for high energy calibration and supervise cross calibration between different missions. This goal is reached through working groups, where IACHEC members cooperate to define calibration standards and procedures. The scope of these groups is primarily a practical one: a set of data and results (eventually published on refereed journals) will be the outcome of a coordinated and standardised analysis of references sources (“high-energy standard candles”). Past, present and future high-energy mission can use these results as a calibration reference.*” (excerpt from the IACHEC web page). In the genetic code of the IACHEC it is imprinted the goal of providing future missions with a testbed of consolidated experiences and good practises, that can be beneficial in designing an optimising in-flight calibration plans.

Regrettably, calibration of X-ray astronomy instrumentation cannot rely on “standard candles” *strictu sensu, i.e.* on sources whose absolute flux is known once other astrophysical observables are measured. One has to be content with sources for which an educated guess of the physical process responsible for their X-ray emission is available. These X-ray “standard candles” exhibit non-thermal broad-band spectra, or thermal spectra in the soft X-ray band. For each source in this set of “standard candles”, the IACHEC aims at defining: a) data reduction and analysis procedures; b) a reference astrophysical model, and publish them, ideally on refereed journals.

In this document I review the in-flight calibration plans of all the missions active in the IACHEC context (basically, all the operational X-ray observatories from the 90s of the past century to now). The document is primarily based on a systematic analysis of the presentations on the calibration status of operational missions routinely held at the yearly IACHEC plenary meetings. These presentations are publicly available at the IACHEC web page:

<http://web.mit.edu/iachec/meetings/index.html>. The *Chandra* Calibration Plan is available

Table 1: Main sources used for the calibration of the LSF and wavelength scale in high-resolution detectors

Source	LETG	HETG	RGS
Capella	X	X	X
HR1099		X	X
Procyon	X		X

at: http://cxc.harvard.edu/newsletters/news_10/CAL.html. The XMM-Newton Routine Calibration Plan is available at: <http://xmm2.esac.esa.int/docs/documents/CAL-PL-0001.pdf>.

2 A synoptic view of in-flight calibration plans

2.1 High-resolution LSF and wavelength scale

Spectra of X-ray bright cool stars have been used for the calibration of the LSF and wavelength scale in the *Chandra*/gratings and the XMM-Newton/RGS (Tab. 2.1): ABDor, Algol, Capella, HR1099, and Procyon (Ness et al. 2002; Fig. 1). Capella is on the average the brightest, and the least variable in this sample: its historical RGS light curve (Capella has been observed yearly by XMM-Newton since the beginning of the mission) exhibits a dynamical range of $\pm 15\%$ (Andy Pollock, private communication). ABDor and HR1099 exhibit large flaring activities, with flux changes of up to one order of magnitude on time scales as short as few hours (see, *e.g.* Audard et al. 2000; Lalitha et al. 2013).

The soft spectrum of these stars cannot cover adequately the whole X-ray spectral bandpass. This is particularly important for the future calibration of the micro-calorimeter on-board Astro-H at the astrophysically crucial iron atomic transitions at 6–7 keV. X-ray binaries with strong unresolved Fe K_α emission lines (*i.e.*, unaffected by Compton or relativistic broadening) would be adequate for this purpose, as well as spectra of X-bright compact SNR or galaxy clusters. Among the former, the HMXRB GX301-2 exhibits a strongly absorbed ($N_H \geq 10^{24}$ cm $^{-2}$) continuum spectrum with a high Equivalent Width Fe K_α fluorescent line, alongside its K_β and fluorescence from neutral states of elements from S to Ni (Fürst et al. 2011). Another potential target in this respect is IGRJ16318-4848 (Matt & Guainazzi 2003)

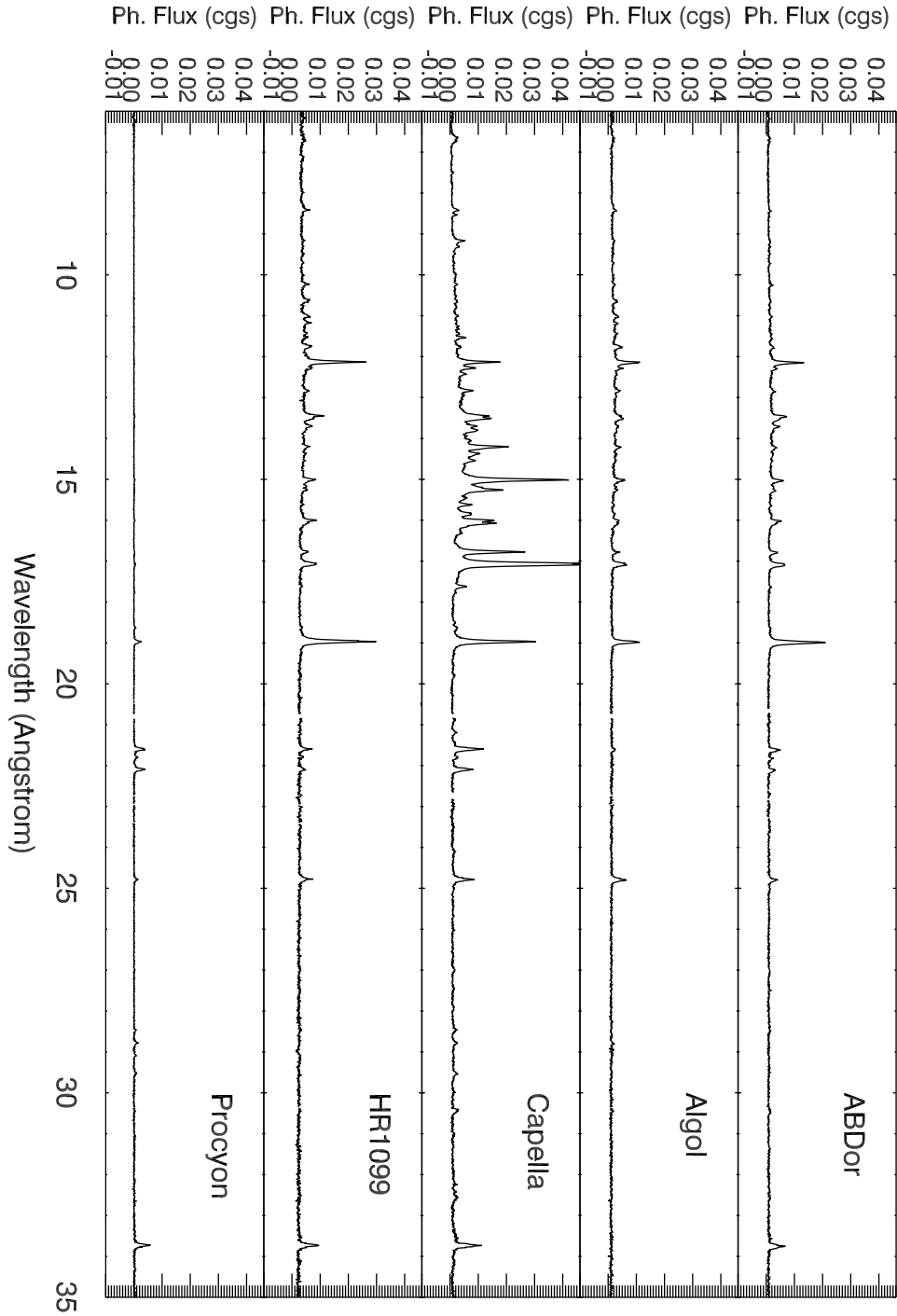


Figure 1: RGS spectra from the longest XMM-Newton observation of five cool stars used for the calibration of the LSF and wavelength scale. The spectra are displayed in on the same linear scale on the y-axis to ease comparison.

Table 2: Main sources used for the calibration of CTI, gain, and redistribution in CCD X-ray detectors

Source	ACIS	EPIC-MOS	EPIC-pn	XIS	XRT
1E0102-72	X	X	X		X
3C273		X			X
CasA	X	X	X		X
Cygnus Loop				X	
Perseus Cluster		X		X	
PKS2155-304		X			X
RXJ1856.5-3754		X			X
Tycho SNR		X	X		X
Vela PWN			X		
ζ Puppis		X	X		
ζ Orionis		X	X		

2.2 CCD redistribution, resolution and energy scale

While the redistribution shape can be in principle adequately characterised by illuminating the cameras with monochromatic beams on ground, spectral degradation induced by various form of radiation damage required a recalibration of the photon redistribution alongside the energy scale (CTI and gain) in several X-ray space detectors. A list of the main targets used for this purpose is given in Tab. 2.2.

Characterisation of the CTI requires uniform illumination of the whole CCD with a source of known spectra, ideally with well isolated (at CCD resolution) atomic transitions. In the EPIC cameras a specific position of the filter wheel (`CAL_CLOSED`) let a ^{55}Fe source shine through the whole field-of-view. Similarly, a ^{55}Fe sources is shone onto the ACIS field-of-view before and after each passage through the radiation belt. The decreasing source flux, the different illumination conditions when compared with typical astronomical background, and the limited spectral range where the ^{55}Fe produces atomic transitions require to complement these measurements with observations of extended sources with strong and well isolated (at CCD resolution) atomic transitions. Vela PWN covers the whole $\simeq 30'$ side EPIC field-of-view, and it has been extensively used by the EPIC calibration team to calibrate the readout losses (see, *e.g.*, Dennerl & Saxton 2012). Strong galaxy clusters such as Centaurus or Perseus have corroborated the calibration results (Gastaldello 2013). Calibration sources in XIS and XRT shine permanently, however covering only a small fraction of the field of view. Large scale sources such as the Cygnus Loop ($\simeq 3^\circ$), Puppis A ($50' \times 60'$), or observations of the bright Earth have been used by XIS for CTI measurements. The characterisation of transfer losses in the central area of the XRT made use of compact X-ray bright SNR such as Cas A, IC443,

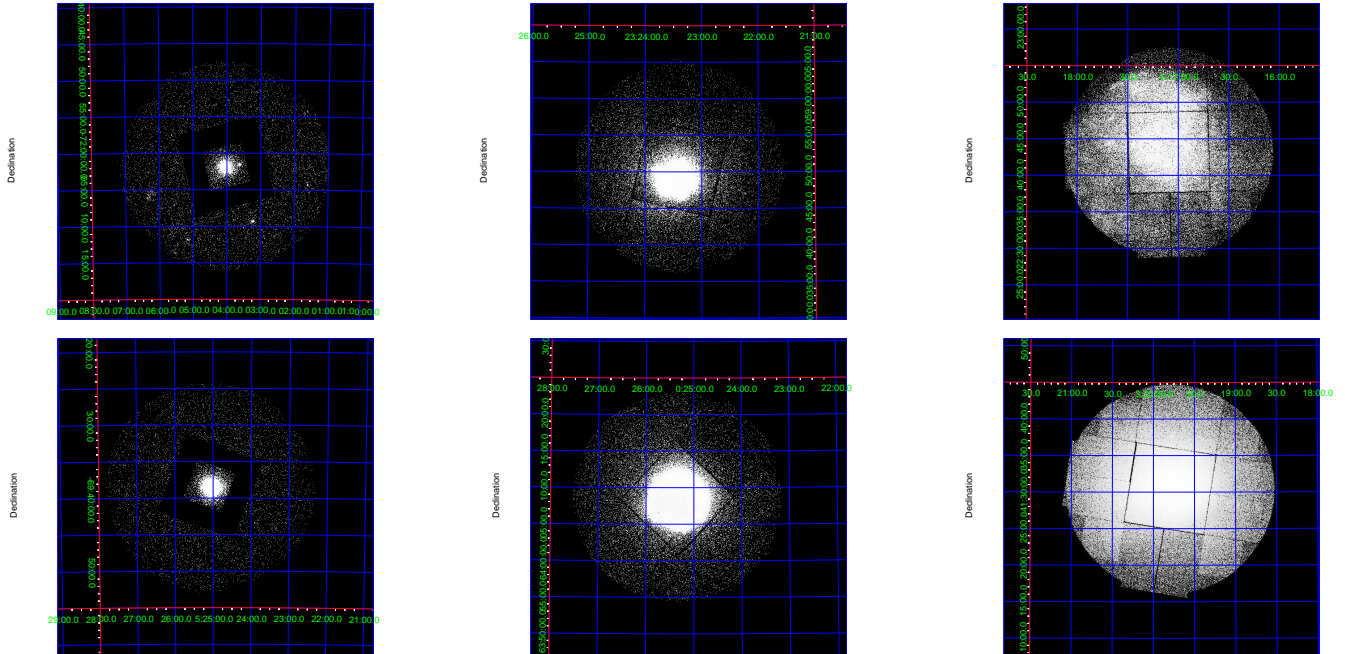


Figure 2: EPIC-MOS2 image of the deepest XMM-Newton observation of five SNR and one galaxy cluster used for calibration of the energy scale and redistribution in X-ray astronomy CCD detectors. *From left to right, top:* 1E0102-72, CasA, IC443; *bottom:* N132, Tycho, and the Perseus galaxy cluster.

or Tycho. Tycho is also one of the targets used to map traps in the EPIC-MOS. A compilation of EPIC-MOS images of SNRs is shown in Fig. 2 showing examples of compact ($<2'$), intermediate ($\simeq 5'$), and large ($\gtrsim 30'$) sources used for calibration purposes.

The study of spectral degradation in space also requires bright, constant sources with well isolated (at CCD resolution) atomic transitions. CasA is an historical choice for ACIS due to its brightness (Fig. 3), also at the Fe energies (see Marsden 2013 for the application to NuSTAR). The mostly used and studied source in the IACHEC context is, however, the compact ($\simeq 1'$ diameter) SNR 1E0102-72.3. The combination of symmetric morphology, lack of Fe-lines, strong and well isolated OVII, OVIL, NeIX, and NeX emission lines, detailed empirical and astrophysical modelling, and deep available observations with all major operational CCD in space (together with a flux constant at a level of better than 1% in all knots; Frank Haberl, private communication) make of 1E0102-72.3 a widely used “standard candle” in soft X-ray astronomy (Plucinsky et al. 2012). Stars like ζ Puppis and ζ Orionis offer alternatively strong NV lines. Very soft continuum sources such as the INs RXJ0720.4-32.5 or RXJ1856.6-3754 offer complementary information thanks to their simple blackbody-like spectrum (Burwitz et al. 2003), and - at least for the latter source - extreme stability (Sartore et al. 2012; source flux variation at the level of a few percent cannot be ruled out yet, Pollock & Guainazzi in preparation). Additional calibration of the redistribution can be

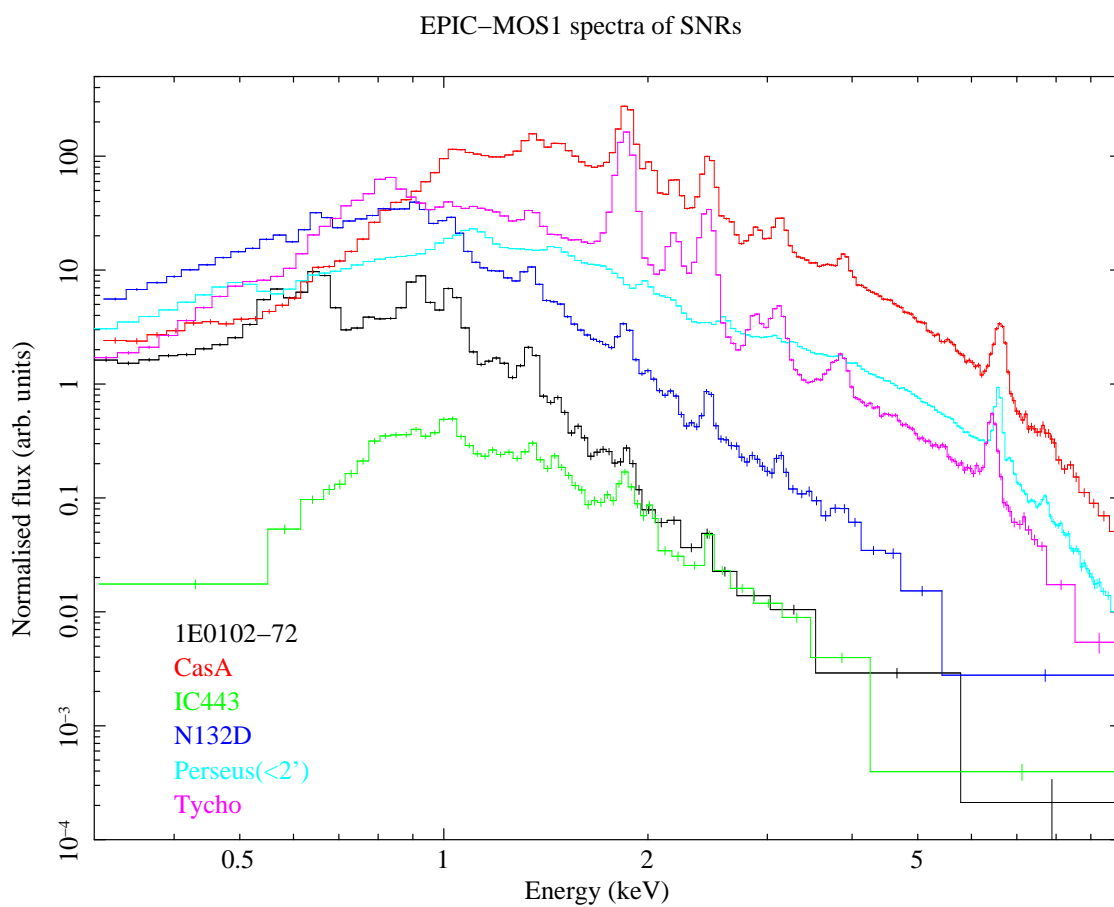


Figure 3: EPIC-MOS1 spectra of SNR and galaxy clusters used for CCD redistribution calibration

Table 3: Main sources used for the calibration of the effective area below 10 keV

Source	HRC	LETG	HETG	RGS	XRS	ACIS	EPIC-MOS	EPIC-pn	GSC	SSC	JEM-X	PCA	XIS	XRT
1E0102-72						X	X						X	X
3C273		X	X		X									X
Abell1795		X				X							X	X
Abell2029		X				X								X
Crab Nebula				X					X	X	X	X		X
G21.5-0.9	X					X								X
H1426+428			X											X
HZ43	X	X												
Mkn421	X	X	X	X										X
Perseus Cluster							X	X						
PKS2155-304	X	X	X	X									X	
RXJ1856.5-3754		X		X									X	X

achieved by looking at the agreement between data and models in bright power-law sources at energy ranges where the effective area exhibit the steepest gradients. GBH binaries such as LMCX-3, or radio-loud AGN such as 3C273 and PKS2155-304 have been used for this purpose.

Finally, it is worth mentioning the possibility of using heavily obscuring sources to constrain the redistribution shelves. This is a particularly promising approach for CCD “Fast Modes” (EPIC-pn Timing and Burst Mode, XRT Window Timing Mode, or the Continuous Clocking Mode in ACIS). Extremely bright obscured binaries can in principle provide an almost uncontaminated view of photons redistributed below 2 keV. The main astrophysical issue is disentangling possible sources of soft excess such as dust-halo scattering, or coronal emission. The IACHEC CCD WG has proposed a pilot coordinated experiment on Cyg X-3, still under approval.

2.3 Area at energies <10 keV

Given the intrinsic degeneracy between redistribution and effective area calibration of CCD in the soft energy band ($\lesssim 1$ keV), the most commonly used sources for the in-flight calibration of the soft X-ray effective area are largely coincident with those used for the calibration of the redistribution (Tab. 2.3). Compact SNR (1E0102-72.3), active stars with well isolated He-like and H-like emission line complexes (ζ Puppis; ζ Orionis), or and very soft INS (RXJ1856.6-3754). In the EUV/extreme soft X-ray band, White Dwarfs such as Sirius B, GD153 or HZ43 have been used to create empirical adjustments to the effective area (Burwitz 2013).

In the hard CCD-band, radio-loud AGN such as 3C273, H1426+128, and PKS2155-304 are still widely used for effective area calibration. A cross-calibration campaign on PKS2155-304 (now involving *Chandra*, NuSTAR, *Suzaku*, *Swift*, and XMM-Newton) has been running continuously since 2006, with one observation every year. However, radio-loud AGN, and in particular blazars (Mkn421, PKS2155-304) are rapidly variable sources, with a complex flux-dependent spectral variability. *Chandra* and XMM-Newton CCDs observations of these objects are almost invariably affected by pile-up. Mitigation actions in the latter case involve excising the PSF core from the spectral accumulation region, yielding additional uncertainties in the spectral deconvolution due to the Encircled Energy Fraction of the PSF wings (Read et al. 2011). The usage of serendipitous catalogues for effective area calibration and cross-calibration has been proposed as a possible alternative (Mateos et al. 2009; Read et al. 2014).

Plerionic spectra may represent a promising alternative (besides the Crab, still used for the calibration of the RXTE/PCA, the NuSTAR instruments, and the instruments on-board MAXI, among others). The IACHEC study on G21.5-0.9 (Tsujimoto et al., 2011) is currently the largest published cross-calibration study ever in terms of number of instruments involved, covering the whole energy band from 2 to 150 keV (the source is obscured by a column density $\simeq 2 \times 10^{22} \text{ cm}^{-2}$).

2.3.1 A note on galaxy clusters as calibration sources

Contamination has been a primary matter of concern for ACIS, EPIC-MOS and XIS. 1E0102-72.3 and RXJ1856-6.3754, given their stability, have been primary targets for the monitoring of the contamination. Galaxy clusters such as Abell 1795 have been also extensively used (see Kettula et al., 2013 for a discussion of the XIS case). Abell 1795 has been used to monitor the spatial distribution of the contaminant in ACIS (David 2013, Marshall 2012). At the same time, galaxy clusters have assumed the role of a reference “standard candles” in the hard X-ray band, following the pioneer cross-calibration work of the IACHEC Galaxy Cluster WG (Nevalainen et al., 2010; Kettula et al. 2013).

Thanks to their flux stability, simple and well understood physics, and smooth morphology, galaxy clusters are excellent calibrator candidates for the scientific payload on-board Astro-H. The ideal source should have the best combination of X-ray flux, small cool core (in order to ensure the largest possible isothermal area), and extension. These quantities are shown in Fig. 4 for the 11 objects of the Nevalainen et al. (2010) sample (see also Sect. 2.7).

2.4 Area at energies >10 keV

Most of the operational instruments above 10 keV have employed the Crab Nebula as primary calibrator for the effective area. The response of the RXTE/PCA (Shaposhnikov et al. 2012) and NuSTAR has been calibrated solely based on the Crab, assuming “standard values” for the photon index and normalisation of a power-law shape. Weisskopf et al. (2010) showed that some models of

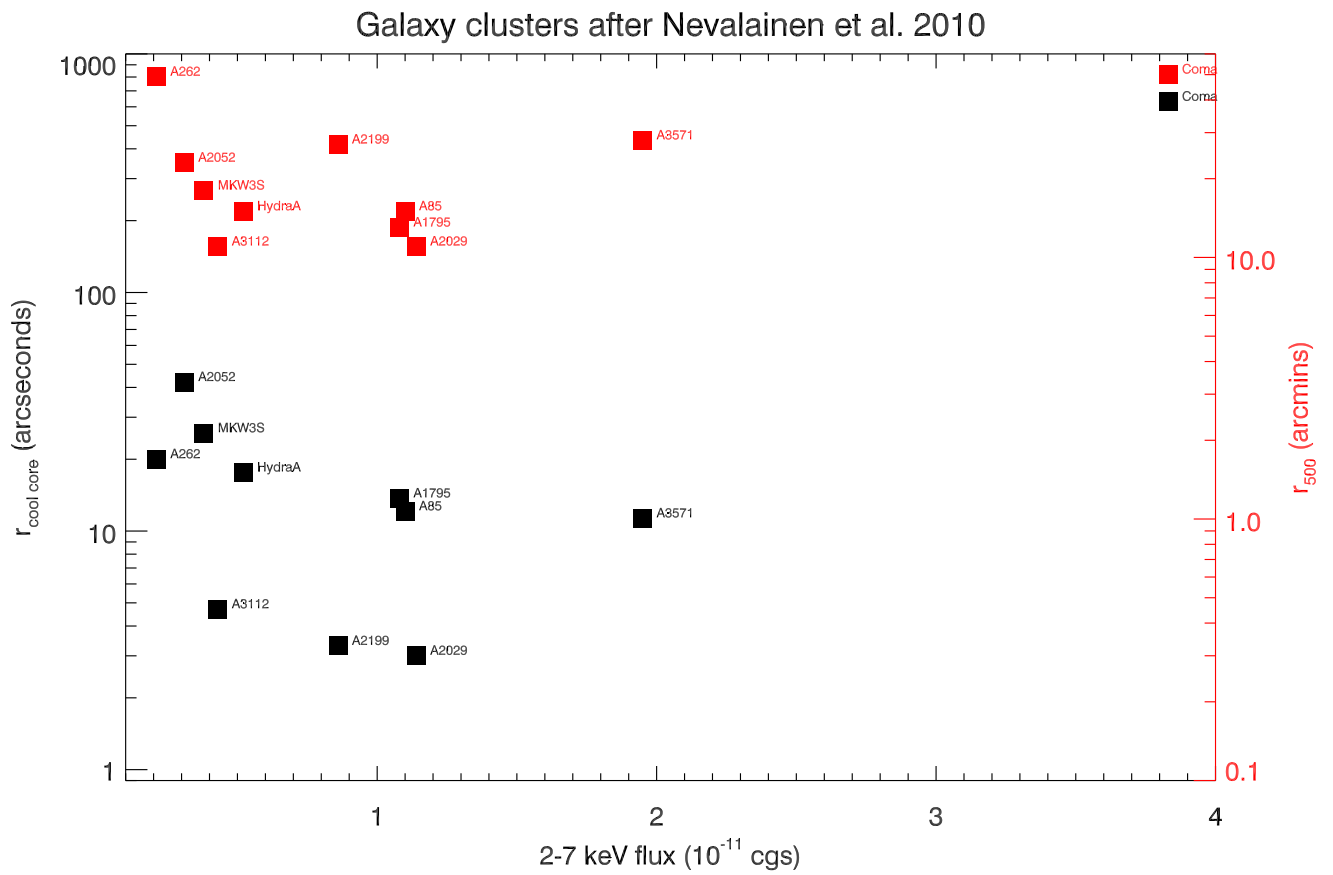


Figure 4: Radius of the cool core ($r_{coolcore}$, black squares, left y-axis), and r_{500} (red squares, right y-axis) as a function of the 2–7 keV flux for the sample of galaxy cluster after Nevalainen et al. (2010)

Table 4: Sources used for the calibration of the effective area above 10 keV

Source	AGILE	BAT	HXD	HEXTE	IBIS	NuSTAR	SPI
Crab Nebula	X ^a	X	X	X	X	X	X
PSR1509-58			X		X		

^aCrab pulsar

the nebula high-energy emission predict a spectral curvature, that should be already measurable by the PCA. This evidence challenges the assumption underlying the calibration of its response. The status of the Crab Nebula as “the standard candle of X-ray astronomy” has been severely undermined by two circumstances: a) the fact that most instruments operating below 10 keV during the first decade of the XXI century could not observe the Crab due to telemetry or pile-up limits, except in special, rarely used instrumental modes; b) the discovery that the Crab is actually a variable source (Wilson-Hodge et al. 2011) exhibiting variations with a dynamical range of $\simeq 7\%$ over the whole X-ray band on time-scales of months (a discovery delayed by the assumption that the Crab Nebula was a stable calibration source!). Alternative plerionic spectra such as G21.5-0.9 and MSH15-52 could yield a statistical accuracy on the determination of the spectra shape of $\Delta\Gamma \sim 0.05$ in a 50 ks observation with the hard X-ray focusing telescopes on NuSTAR and Astro-H. With a NuSTAR observation of 280 ks of G21.5-0.9, the error on the spectral index ($\Delta\Gamma \simeq 0.013$) is comparable to the systematic error due to uncertainties in the effective area calculations (K.Mardsen, private communication). These performances are comparable to those of a bright radio-loud hard AGN such as 3C273. However, 3C273 exhibit a hard X-ray flux historical variability of about 50% (Soldi et al. 2008).

2.5 PSF

“First-light”-like bright sources such as X-ray binaries (CygX-1, CygX-2, HerX-1), stars (ARLac, Capella) or bright AGN (3C273, MCG-6-30-15) have been used for this purpose, depending on the brightness limitations.

2.6 Timing

The Crab pulsar ($\simeq 33$ ms) has been the main target used for timing calibration (Terada et al., 2008; Martin-Carrillo et al., 2012). Alternative targets are discussed in Terada (2009) and Martin-Carrillo et al. (2012): A0535-262 (103 s) AeAqr (33 s), AmHer (11140 s), HerX-1 (1.237 s), PSRB0540-69 (51 ms) PSRJ0537-69 (50 ms), PSRB1055-52 (197 ms), PSRB1509-58 (in MSH15-52; 0.15135 s), Vela pulsar (88 ms)

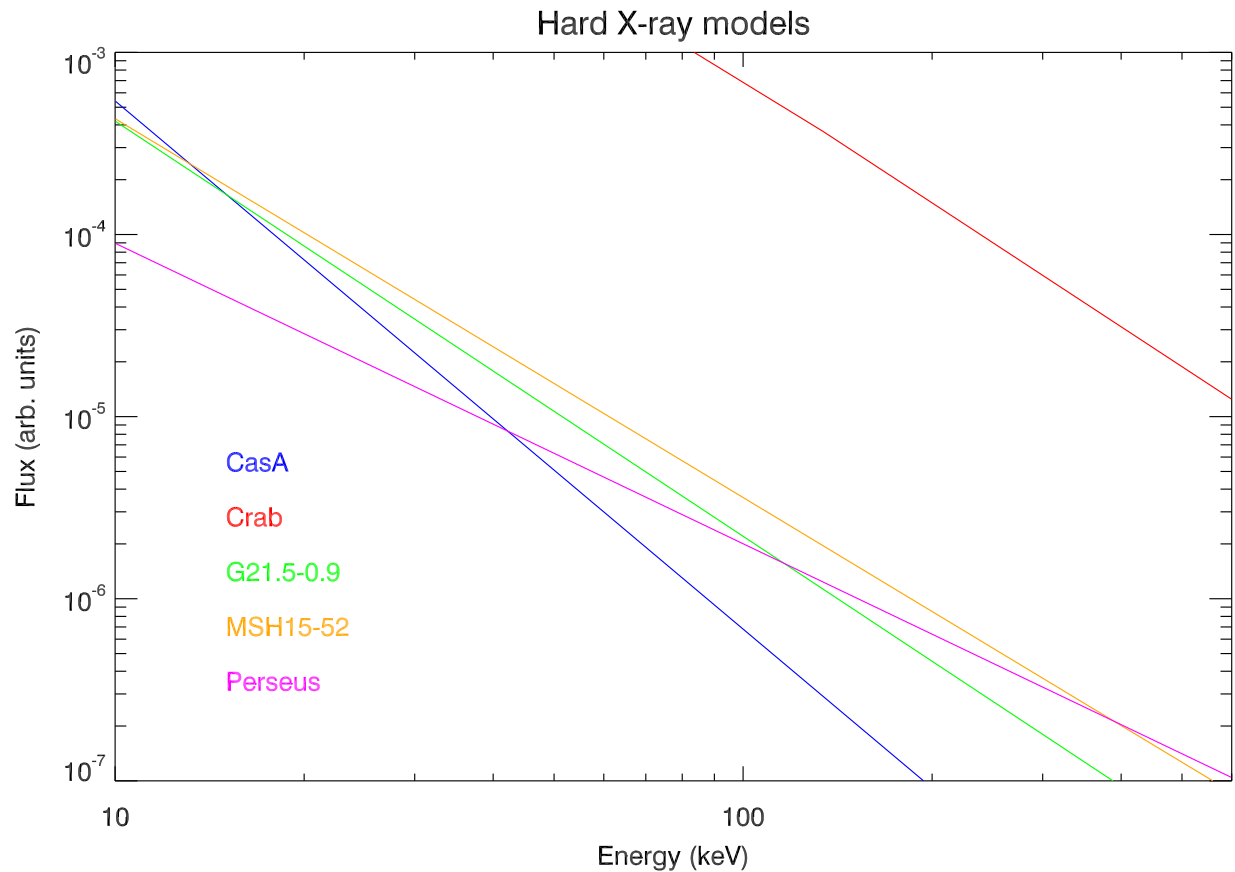


Figure 5: Models of plerionic spectra above 10 keV: Crab (*black*; Kouzu et al. 2013), G21.5-0.9 (*red*; Tsujimoto et al. 2011), MSH15-52 (*green*, Mineo et al. 2001). They are compared to the spectra of the SNR Cas A (*blue*, Vink et al. 2000), and 3C273 in its lowest (*cyan*) and highest (*magenta*) state in the 2003–2005 INTEGRAL and XMM-Newton monitoring (Chernyakova et al. 2007). The numbers in *brackets* indicate the 90% confidence level error on the photon index (one interesting parameter).

2.7 Cross-calibration

Several IACHEC Working Groups¹ have been engaged in defining “standard candle” for cross-calibration purposes:

- **Clusters of Galaxies:** Nevalainen et al. (2010) discuss a sample of bright clusters of galaxies, used for the verification of the cross-calibration status among the operational CCD cameras in the 0.7–10 keV energy band, as well as for the re-calibration of the *Chandra* effective area embedded in the CALDB change between 3.4 and 4.1. The sample is constituted by: Abell 1795, Abell 2029, Abell 2052, Abell 2199, Abell 262, Abell 3112, Abell 3571, Abell 85, Coma, HydraA, MKW3S.
- **Effective area:** This WG has been running since 2006 a cross-calibration campaign on PKS2155-304 (Ishida et al. 2011). This campaign is constituted by simultaneous observations of with *Chandra*, NuSTAR, *Suzaku*, Swift, and XMM-Newton. Other blazars such as 3C273 and H1426+428 are the basis of a systematic comparison of the effective area calibration between the *Chandra* gratings and the XMM-Newton X-ray payload (Smith & Marshall, in preparation)
- **Non-thermal SNR:** This WG deals primarily with effective area cross-calibration above 10 keV. The pioneer work by Kirsch et al. (2005) on the Crab Nebula, has been later challenged (Weisskopf et al. 2010, Wilson-Hodge et al., 2011). An updated of this study, solely based on quasi-simultaneous observations, is being published (Natalucci et al., in preparation). Alternative, albeit weaker, plerionic spectra have been proposed for this purpose, such as G21-5-0.9 (Tsujimoto et al., 2011).
- **Thermal SNR:** The compact SNR 1E0102-72.3 has become a standard calibration target for redistribution and effective area motoring. A semi-empirical model based on a continuum version of the APEC code (Foster et al. 2012) was developed to describe its soft X-ray spectrum, and constrained observationally using the RGS spectra. The 1E0102-72.3 spectra are used to constrain the cross-calibration of the effective area at the energy of strong and well-isolated (at CCD resolution) He- and H-like transitions of OVII, OVIII, NeIX, and NeX (Plucinsky et al. 2012)
- **White Dwarfs and Isolated Neutron Stars:** The main goal of this WG is the refinement of the LETGS effective area in the softest X-ray energy band ($\lambda > 40\text{\AA}$). Sources used for this purpose are WDs such as GD153, Hz43, and Sirius B, as well as the INS RXJ1856-6-3754.

¹<http://web.mit.edu/iachec/wgs>

References

Audard M., et al., 2000, *A&A*, 541, 396

Burwitz V., et al., 2003, *A&A*, 399, 1109

Burwitz V., 2013, presentation at the 8th IACHEC (available at:
http://web.mit.edu/iachec/meetings/2013/Presentations/WD_iNS.pdf)

Chernyakova M., et al., 2007, *A&A*, 465, 147

Dennerl K. & Saxton R., 2012, XMM-CCF-REL-0283 (available at:
<http://xmm2.esac.esa.int/docs/documents/CAL-SRN-0283-1-0.ps.gz>)

David L., 2013, presentation at the 8th IACHEC (available at:
<http://web.mit.edu/iachec/meetings/2013/Presentations/David.pdf>)

Foster A.R., et al., 2012, *ApJ*, 756, 128

Fürst F., et al., 2011, *A&A*, 535, 9

Gastaldello F., 2013, XMM-SOC-CAL-TN-0184 (available at:
<http://xmm2.esac.esa.int/docs/documents/CAL-TN-0184-1-0.pdf>)

Kettula K., et al., 2013, *A&A*, 552, 47

Kirsch M., et al., 2005, *SPIE*, 5898, 22

Kouzu T., et al., 2013, *PASJ*, 65, 74

Ishida M., et al., 2011, *PASJ*, 63, 657

Lalitha S., et al., 2013, *ApJ*, 560, 69

Matt G., Guainazzi M., 2003, *MNRAS*, 341, L13

Mineo T., et al., 2001, *A&A*, 380, 695

Mardsen K., 2013, presentation at the 8th IACHEC (available at:
<http://web.mit.edu/iachec/meetings/2013/Presentations/Mardsen.pdf>)

Marshall H., 2012, presentation at the 7th IACHEC (available at:
<http://web.mit.edu/iachec/meetings/2012/Presentations/Marshall.pdf>)

Martin-Carrillo A., et al., 2012, A&A, 545, 126

Mateos S., et al., 2009, A&A, 496, 879

Ness J.-U., et al., 2002, ApJ, 394, 911

Nevalainen J., et al., 2010, A&A, 532, 22

Plucinsky P.P., et al., 2012, SPIE, 8443, 12

Read A.M., 2005, ESA-SP-604

Read A.M., 2011, A&A, 543, 34

Read A.M., 2014, A&A, 564, 45

Sartore N., et al., 2012, A&A, 541, 66

Sembay S., et al., 2010, AIPC, 1248, 593

Shaposhnikov N., et al., 2012, ApJ, 757, 159

Soldi S., et al., 2008, A&A, 486, 411

Terada Y., et al., 2008, PASJ, 60, 25

Terada Y., 2009, presentation given at the 5th IACHEC meeting (available at:
<http://web.mit.edu/iachec/meetings/2009/Terada.pdf>)

Tsujimoto M., et al., 2011, A&A, 525, 25

Vink J., et al., 2000, AdSpR, 25, 689

Weisskopf M., et al., 2010, ApJ, 713, 912

Wilson-Hodge C.A., et al., 2011, ApJ, 727, 40